

What if your Chemistry research received 2x the citations and 3x the amount of downloads?



The benefits for you as an author publishing open access are clear: Articles published open access have wider readership and are cited more often than comparable subscription-based articles.

Submit your paper today.



DOI:10.1002/ejic.201300419

Unveiling the Interaction of Vanadium Compounds with Human Serum Albumin by Using ^1H STD NMR and Computational Docking Studies

David M. Dias,^[a] João P. G. L. M. Rodrigues,^[b]
 Neuza S. Domingues,^[a] Alexandre M. J. J. Bonvin,^[b] and
 M. Margarida C. A. Castro^{*[a,c,d]}

Keywords: Proteins / Docking studies / Drug delivery / Vanadium / NMR spectroscopy

The binding of the V^{V} oxidation products of two vanadium(IV) compounds, $[\text{VO}(\text{dmpp})_2]$ and $[\text{VO}(\text{maltolato})_2]$, which have shown promising anti-diabetic properties, to human serum albumin (HSA) in aqueous aerobic solution has been studied by ^1H saturation transfer difference (STD) NMR spectroscopy and computational docking studies. Group epitope mapping and docking simulations indicate a preference of HSA binding to the 1:1 $[\text{VO}_2(\text{dmpp})(\text{OH})(\text{H}_2\text{O})]^-$ and 1:2 $[\text{VO}_2(\text{maltol})_2]^-$ vanadium(V) species. By using known HSA binders, competition NMR experiments revealed that both

complexes preferentially bind to drug site I. Docking simulations carried out with HADDOCK together with restraints derived from the STD results led to three-dimensional models that are in agreement with the NMR spectroscopic data, providing useful information on molecular interaction modes. These results indicate that the combination of STD NMR and data-driven docking is a good tool for elucidating the interactions in protein–vanadium compounds and thus for clarifying the mechanism of drug delivery as vanadium compounds have shown potential therapeutic properties.

Introduction

Over the last few years vanadium compounds (VCs) have attracted considerable interest from the scientific community due to their demonstrated pharmacological properties.^[1] In particular, their potential use as oral insulin mimetic agents has been demonstrated by *in vivo*^[2,3] and *ex vivo* studies^[4] as well as in clinical trials.^[5] Their insulin-like capacity to modulate several metabolic pathways may be due to their inhibitory effect on protein tyrosine phosphatases (PTPases) and/or the activation of tyrosine kinases, which are responsible for the activation of signal transduction pathways, particularly in the insulin signalling cascade.^[6] Intensive research has been carried out to develop VCs for use as orally administered drugs in the treatment

of Type II diabetes mellitus (DM) at an effective non-toxic dose. Among the many compounds synthesized to date, only a few seem to show promise for this purpose. Bis(maltolato)oxovanadium(IV) (BMOV),^[7] bis(picolinato)oxovanadium(IV) and bis(allixinato)oxovanadium(IV) as well as other derivatives^[8] have demonstrated anti-diabetic properties^[9–11] through indicators of insulin mimetism assessed by *in vitro* and *ex vivo* studies such as glucose uptake rates,^[12,13] inhibition of free fatty acid (FFA) release^[14] and specific protein phosphorylation.^[4,10] *In vivo* experiments have confirmed their therapeutic activity and toxicity,^[15,16] established the minimum effective dose^[17] and provided information about bioavailability and pharmacokinetics. BMOV and similar compounds like bis(ethylmaltolato)oxovanadium(IV) (BEOV) have already been presented in clinical trials.^[18]

The vanadium complex bis(3-hydroxy-1,2-dimethyl-4-pyridinonato)oxovanadium(IV), $[\text{V}^{\text{VO}}(\text{dmpp})_2]$, has been extensively studied. Its structure in the solid state has been determined^[19] and the different species formed in aqueous solution under aerobic conditions were identified by using different techniques and the respective formation constants determined.^[20] *In vitro* insulin mimetic and toxicity studies with two cell lines, the mouse fibroblast SV 3T3 and the human skin fibroblast F26,^[21] have been conducted. Studies with the human fibroblast cell line, 3T3-L1,^[15] as well as with human erythrocytes^[22] have also been carried out to test its cytotoxicity and glucose uptake enhancement ca-

[a] Department of Life Sciences, Faculty of Sciences and Technology, University of Coimbra, P. O. Box 3046, 3001-401 Coimbra, Portugal
 E-mail: gcastro@ci.uc.pt
 Homepage: www.uc.pt/ftctuc/dcv

[b] Bijvoet Center for Biomolecular Research, Department of Chemistry, Faculty of Science, Utrecht University, Padualaan 8, 3584 CH Utrecht, The Netherlands

[c] Coimbra Chemistry Centre, Rua Larga, University of Coimbra, 3004-535 Coimbra, Portugal

[d] Center of Neurosciences and Cell Biology, University of Coimbra, 3001-401 Coimbra, Portugal

Supporting information for this article is available on the WWW under <http://dx.doi.org/10.1002/ejic.201300419>.

capacity. Recently, its anti-diabetic action was recognized through an *ex vivo* study with isolated primary rat adipocytes, which demonstrated that this compound improves glucose internalization, inhibition of FFA release, and has the capacity to activate the insulin signalling cascade through phosphorylation of the key proteins of this pathway.^[23] *In vivo* studies with obese Zucker rats by using magnetic resonance techniques (MRI/MRS) confirmed the positive effects of $[V^{IV}O(dmpp)_2]$ on glucose and lipid metabolism, reinforcing its promising anti-diabetic capacity.^[24]

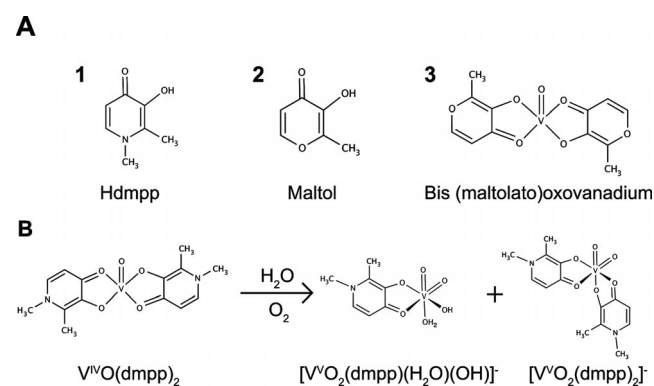
However, the mechanism of the therapeutic action of VCs in the human body has not yet been clarified. The increased pharmacological effect of chelated V^{IV} complexes compared with $VOSO_4$ has been attributed, in part, to increased absorption in the gastrointestinal tract.^[25] The differences in biodistribution and efficacy observed between non-chelated and chelated vanadyl ions result from a small portion of the administered complex remaining intact after absorption.^[21,26] A major concern is how this intact fraction of the VCs is transported in the blood stream and is taken up by the cells of peripheral tissues.^[27] Thus, it is important to know the interactions between the administered VCs and endogenous macromolecular components and/or small bioligands (such as lactate and citrate) present in blood serum to determine whether the decomposition of the VCs occurs or ternary complexes are formed, and to investigate the role of serum proteins in the transport of VCs.^[28–34] This information is crucial in the search for a rational drug design to improve the therapeutic efficacy of these compounds.

The two main serum proteins involved in the transport of vanadium species (both V^{IV} and V^V) are human serum transferrin (Tf) and albumin (HSA). The interaction of vanadyl (V^{IV}) and vanadate (V^V) with transferrin has been detected by different techniques, including gel electrophoresis, ultrafiltration, chromatographic techniques, atomic absorption spectrometry (AAS) and inductively coupled plasma mass spectrometry (ICP-MS).^[35,36] Structural information on these interactions was obtained by spectroscopic techniques, such as UV/Vis and FTIR and FT Raman spectroscopy.^[37] Vanadate binds to the two Fe^{III} binding sites of apo-transferrin as the dioxovanadium(V) cation, VO_2^+ , to form a $(VO_2^+)_2$ -Tf complex without the need of a synergistic binding anion, as shown by ^{51}V NMR spectroscopy,^[38] whereas apo-transferrin requires such a synergistic cation to bind two equivalents of the oxidovanadium(IV) cation, VO_2^{2+} , at these sites.^[39] HSA strongly binds one equivalent of VO_2^{2+} in the Cu^{II} site at the N terminus and several equivalents, weakly and non-specifically, to carboxylate side-chains of surface amino acids.^[40] However, when the VO_2^{2+} /HSA ratio is 1:1 or lower, a binuclear metal species, $(VO_2^+)_2$ -HSA, is formed.^[29] EPR spectroscopy was used as an essential tool of such extensive interaction studies of VO_2^{2+} with Tf and HSA.^[28,29,41] It is not yet fully clear in which form the VO_2^{2+} ion is transported to the target cells in the organism as the higher concentration of HSA in the blood could compensate its much lower affinity towards VO_2^{2+} relative to transferrin.^[42] In addition, the competition

effects of small bioligands present in the serum also need to be taken into consideration.^[29]

The interaction of V^{IV} compounds, including BMOV and $[VO(dmpp)_2]$, with apo-Tf, HSA and small bioligands present in blood serum has been studied by EPR and circular dichroism (CD).^[27–34,43] The results indicate that, besides the case in which the binding of the carrier ligand to vanadium is very weak, for example, 6-methylpicolinate, mixed species are formed with transferrin with possible partial carrier ligand displacement, to form *cis*- $[VO(carrier)_x(Tf)]$ species ($x = 1, 2$; carrier ligand = picolinate, maltolato, dmpp). In the case of HSA, mixed species *cis*- $[VO(carrier)_2(HSA)]$ involving hydrogen bonding and/or hydrophobic interactions with the protein surface have also been proposed.

The formation of ternary species between the proteins and the VO-carrier complex is an important issue as it affects the distribution of species in the blood plasma. Therefore independent evidence of their presence was an important objective of this work. Although it is usually accepted that the metal ion is transported in the blood in the V^{IV} oxidation state,^[27,44] almost independently of the initial oxidation state of the VC, oxidation may occur, resulting in the formation of a limited amount of diamagnetic V^V species, which can be studied by NMR spectroscopy. In this work we studied the interaction in aqueous solution of vanadate/Hdmpp complexes with HSA by using the 1H saturation transfer difference (STD) NMR technique.^[45] This technique provides data on the interaction of small molecules with a protein, validation of binding epitopes, estimation of affinity constants and site-specific information through competition studies. The vanadate/Hdmpp (M/L = 1:2) solution contains both 1:1 and 1:2 V^V species (Scheme 1), the same species that result from the dissolution of the solid $[V^{IV}O(dmpp)_2]$ in water under aerobic conditions.^[20]



Scheme 1. A) Chemical structures of 3-hydroxy-1,2-dimethyl-4-pyridinone (**1**, Hdmpp), 3-hydroxy-2-methyl-4-pyrone (**2**, Maltol) and bis(maltolato)oxovanadium(IV) (**3**, BMOV) (with $K_1 = 107.5$ and $K_2 = 106.2$). B) Chemical equilibrium representing the dissolution of the solid bis[3-hydroxy-1,2-dimethyl-4-pyridinonato]oxovanadium(IV), $[V^{IV}O(dmpp)_2]$ in H_2O under physiological conditions and the resulting oxidation products, the vanadium(V) species $[V^{V}O_2(dmpp)(H_2O)(OH)]^-$ and $[V^{V}O_2(dmpp)_2]^-$, with M/L ratios of 1:1 and 1:2, respectively (with $K_1 = 1010.48$ and $K_2 = 105.25$).

The use of the diamagnetic vanadate/Hdmpp system instead of an aerobic solution of $[V^{IV}O(dmpp)_2]$ avoids the presence of a small amount of paramagnetic species in solution resulting from incomplete oxidation,^[20] which would not allow the correct use of 1H STD NMR experiments. Competitive 1H STD NMR experiments with two known inhibitors of site I and site II of HSA, warfarin and ibuprofen, respectively (for a definition of site I and site II see the Supporting Information), were performed to discriminate the preferential binding site of the V^V coordinated species and Hdmpp.^[46] A parallel study was also carried out with the vanadate/maltol system to investigate the behaviour of the $[V^{IV}O(maltolato)_2]$ compound (Scheme 1). The STD results were complemented by data-driven docking calculations performed with HADDOCK,^[47,48] taking into account the information from STD experiments, resulting in 3D models that illustrate the interaction of V^V species with HSA, one of the main plasma proteins. Herein we show that this procedure is a useful tool for providing important information on drug delivery, an approach not previously employed in the study of the use of vanadium compounds as therapeutic drugs.

Results and Discussion

Figure 1 presents the 1D 1H NMR spectra of solutions containing 5 mM free Hdmpp (A), vanadate/Hdmpp (1:2, 1 mM in vanadate) in the presence of 0.03 mM HSA (B) and the 1H STD spectrum of solution B (C).

Spectrum A shows the signals corresponding to the two methyl groups and the aromatic 5-H and 6-H protons, assigned in accordance with the literature.^[20] In the spectra of solutions containing 1:2 vanadate/dmpp, multiple signals are observed for each type of proton, which have been assigned in the figure, indicating the presence in solution of three main species in slow exchange on the NMR timescale:

the free dmpp and two vanadium(V) complexes, the 1:1 $[VO_2(dmpp)(H_2O)(OH)]^-$ and 1:2 $[VO_2(dmpp)_2]^-$ V^V species (Scheme 1). When HSA was added to the vanadate/dmpp system (spectrum B), the resonances of dmpp in all species broaden and lose resolution, as expected, due to their interaction with the protein and the small increase in solution viscosity. Only signals of the small molecules are observed as the protein resonances were suppressed by using a spin-lock filter during the acquisition.

A similar study was carried out with the vanadate/maltol system and the 1H NMR signals of the obtained spectra are assigned in Figure 2, in agreement with literature data^[49] and as confirmed by 1H NMR spectra obtained from solutions of vanadate/maltol at different metal/ligand (M/L) ratios (data not shown).

In the spectrum of vanadate/maltol, M/L = 1:2, two signals for the methyl group and the 5-H and 6-H aromatic protons are observed corresponding to free maltol and the 1:2 V^V complex, $[VO_2(maltolato)_2]^-$ (Scheme 1), in slow exchange on the NMR timescale.^[49] Again for this system, all the resonances broaden in the presence of HSA (Figure 2, B), reflecting the binding of maltol and $[VO_2(maltolato)_2]^-$ to the protein and the small increase in the viscosity of the solution. The relative intensities of the resonances of the species detected in solution for the two systems are in agreement with the values of the formation constants determined for the 1:1 and 1:2 complexes in both systems. Whereas in the vanadate/Hdmpp system the association constants for the 1:1 and 1:2 species are, respectively, $K_1 = 1010.48 M^{-1}$ and $K_2 = 105.25 M^{-1}$,^[20] in the vanadate/maltol system the corresponding association constants are $K_1 = 107.5 M^{-1}$ and $K_2 = 106.2 M^{-1}$.^[49]

Figure 1 (C) shows the 1H STD NMR spectrum of the solution containing vanadate/dmpp (1:2) and HSA. The appearance of the resonances of the three species L, VL and VL_2 in the spectrum indicates, qualitatively, that all these

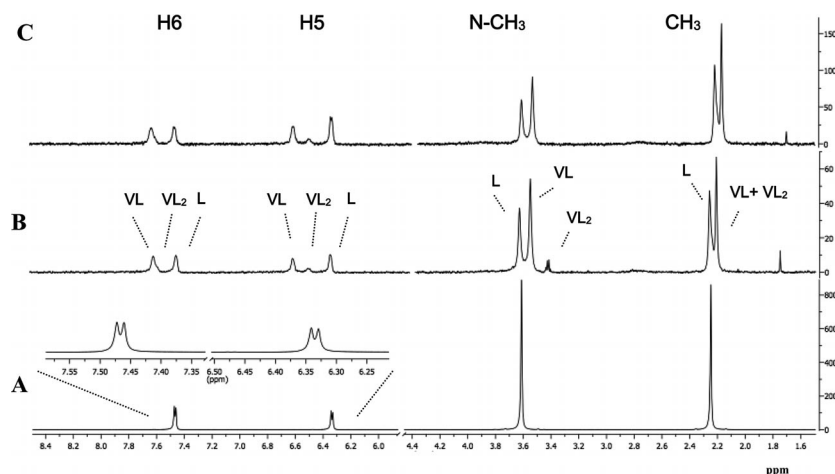


Figure 1. 1H NMR spectra of A) an aqueous solution of 5 mM Hdmpp, B) an aqueous solution of vanadate/Hdmpp (1 mM in vanadate) in an M/L ratio of 1:2 with 30 mM HSA at pH = 7 and C) STD NMR spectrum of solution (B). A spin-lock pulse of 30 ms was used to remove protein resonances. The signal assignments are shown in the figure: L is the free Hdmpp and VL and VL_2 are the 1:1 $[VO_2(dmpp)(H_2O)(OH)]^-$ and 1:2 $[VO_2(dmpp)_2]^-$ complexes, respectively. The difference in the vertical scale of the reference (A,B) and STD (C) spectra is due to the different number of scans used in the respective acquisitions (see the Exp. Sect.).

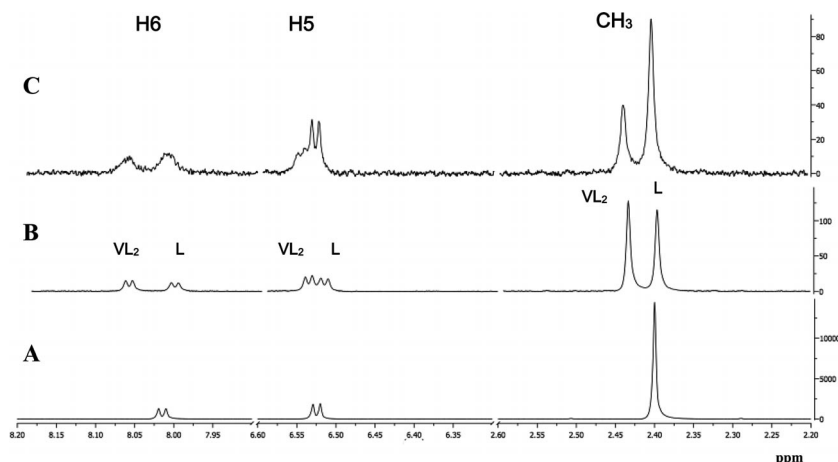


Figure 2. ^1H NMR spectra of A) an aqueous solution of 60 mM maltol, B) an aqueous solution of vanadate/maltol (1 mM in vanadate) in an M/L ratio of 1:2 with 30 mM HSA at pH = 7 and C) STD NMR spectrum of solution B. A spin-lock pulse of 30 ms was used to remove protein resonances. The signal assignments are shown in the figure: L is the free maltol and VL and VL₂ are the 1:1 $[\text{VO}_2(\text{maltolato})(\text{H}_2\text{O})(\text{OH})]^-$ and 1:2 $[\text{VO}_2(\text{maltolato})_2]^-$ complexes, respectively. The difference in the vertical scale of the reference (A,B) and STD (C) spectra is due to the different number of scans used in the respective acquisitions (see Exp. Sect.).

species bind to the protein. However, only through an integration of the signals in spectra B and C and the determination of the corresponding A_{STD} values [by using Equations (1) and (2), see the Exp. Sect.] is it possible to draw conclusions about the relative binding strengths of the different species to the protein and to identify the group epitope for each one by group epitope mapping (GEM). The A_{STD} values allowed full GEM characterization of the vanadate/Hdmpp system (Table 1).

Table 1. Values of GEM relative to the highest values of A_{STD} (5-H of the 1:1 species and 6-H of the 1:2 species for vanadate/Hdmpp and vanadate/maltol systems, respectively) obtained from the interaction of all the small molecules with HSA.

Small molecule	GEM [%]			
	6-H	5-H	CH ₃	N-CH ₃
Hdmpp	75	82	61	42
$[\text{VO}_2(\text{dmpp})(\text{H}_2\text{O})(\text{OH})]^-$	65	100	59	41
$[\text{VO}_2(\text{dmpp})_2]^-$	75	83	59	41
Maltol	79	93	65	–
$[\text{VO}_2(\text{Maltol})_2]^-$	100	97	30	–

In this case, although all the species seem to interact with HSA, the values obtained indicate that there is a slight preference for the binding of the 1:1 species and through the 5-H proton, as this resonance is the highest saturation-receiving proton. The calculated values of GEM for all the Hdmpp protons were normalized relative to the value for 5-H. Similar studies carried out with the vanadate/maltol system (1 mM in vanadate) with M/L = 1:2 in the presence of HSA (0.03 mM) led to the ^1H STD NMR spectrum shown in Figure 2 (C) and the GEM values in Table 1. The presence of all the resonances in the STD spectrum indicates that both free maltol and the 1:2 species bind to the protein. However, according to the GEM values, the strong-

est interaction with HSA occurs through 6-H of the 1:2 species, although a rather similar saturation transfer is observed for 5-H and 6-H.

To investigate the possible binding sites on HSA, competitive ^1H STD NMR studies with the most interactive species were carried out in the presence of warfarin and ibuprofen, two known binders to site I and site II of HSA, respectively.^[50] The displacement of binding species from these sites by the corresponding reported specific inhibitor after being added to the initial solution of vanadate systems and HSA reflects a direct competition and interaction of the species at these sites.^[50]

Integration of the competitive ^1H STD NMR spectra for the vanadate/dmpp (1:1) and HSA solution (Figure 3) led to the A_{STD} values presented in Table 2. It can be concluded that the interaction of the 1:1 complex $[\text{VO}_2(\text{dmpp})(\text{H}_2\text{O})(\text{OH})]^-$ with the binding site I is slightly favoured.

Although displacement of the species from both site I and site II of HSA was observed, according to the A_{STD} values, in the absence and presence of warfarin and ibuprofen, the largest decrease occurs in the presence of warfarin for all the ligand protons of the 1:1 complex, which indicates that binding to site I is favoured over site II. It is also known that ibuprofen displaces species at site I of HSA, albeit to a lesser extent, and so, if the interaction occurs through site II a higher displacement would be expected and reflected by a smaller A_{STD} value.

Similarly, Figure 4 presents typical spectra of the competition studies, through the ^1H STD NMR technique, for the vanadate/maltol (1:2) and HSA system in the presence and absence of warfarin and ibuprofen, and the corresponding A_{STD} values are presented in Table 2.

The results obtained for this system are in agreement with those for the vanadate/Hdmpp system. The A_{STD} values in Table 2 show that, again in this system, greater displacement occurs from site I, as revealed by the larger de-

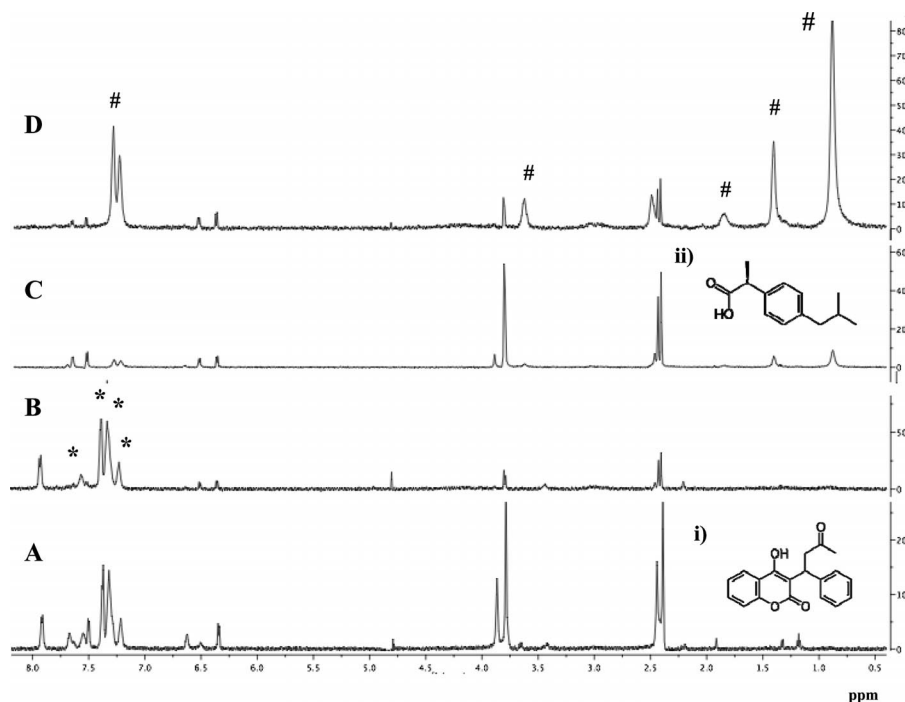


Figure 3. ^1H NMR spectra of A) a solution containing vanadate/Hdmpp (1:2.5, 1 mM in vanadate) and 0.03 mM HSA to which 0.1 mM warfarin (structure i) has been added, B) the STD spectrum of the same solution as in A, C) a solution of vanadate/Hdmpp (1:2.5, 1 mM in vanadate) and 0.03 mM HSA to which 0.4 mM ibuprofen (structure ii) has been added and D) the STD spectrum of the same solution as in C. A selective saturation pulse (5 s) was applied to the 0 ppm region of the protein. A 30 ms spin-lock pulse was calibrated to avoid unwanted protein resonances. In this study, a solution of vanadate/Hdmpp, 1 mM in vanadate and an M/L ratio of 1:2.5 was used to allow the observation of the resonances assigned to the free ligand as well as those of the 1:1 and 1:2 species, and thus to identify the behaviour of the three species relative to protein binding. Competitor resonances are indicated by * (warfarin) and # (ibuprofen). The difference in the vertical scale of the reference (A,C) and STD (B,D) spectra is due to the different number of scans used in the respective acquisitions (see the Exp. Sect.).

Table 2. Values of A_{STD} for all protons of the species $[\text{VO}_2(\text{dmpp})(\text{H}_2\text{O})(\text{OH})]^-$ and $[\text{VO}_2(\text{maltol})_2]^-$, which preferentially bind to HSA, after the addition of 0.4 mM ibuprofen or 0.1 mM warfarin to solutions containing the vanadate/Hdmpp,maltol systems and the protein. The percentage of displacement is reflected by the decrease in the A_{STD} value upon the addition of the inhibitor.

	A_{STD}				Displacement by competition [%]			
	6-H	5-H	CH_3	N- CH_3	6-H	5-H	CH_3	N- CH_3
$[\text{VO}_2(\text{dmpp})(\text{H}_2\text{O})(\text{OH})]^-$	10.67	16.42	9.67	6.73				
vs. Ibuprofen	2.41	2.18	2.36	2.44	77	87	76	64
vs. Warfarin	0.02	0.04	0.03	0.06	99	98	99	99
$[\text{VO}_2(\text{maltolato})_2]^-$	11.7	11.4	3.5	–				
vs. Ibuprofen	6.1	5.8	2.6	–	48	49	26	–
vs. Warfarin	3.4	2.4	1.2	–	71	79	66	–

crease in the A_{STD} values for all the protons of the $[\text{VO}_2(\text{maltolato})_2]^-$ complex in the presence of warfarin. Although these results do not exclude the possibility of binding to any additional sites of the protein not screened in this study,^[50] a common behaviour towards the HSA binding of these V^{V} species with a similar chemical structure is demonstrated, with a slight preference of this type of compound for site I relative to site II.

To complement the STD NMR spectroscopic data with a more detailed structural representation, molecular docking studies were carried out between HSA and each of the V^{V} species (small molecules) by using HADDOCK.^[47,48] Fig-

ure 5 shows the 3D docking models for the binding of the small molecules under study to HSA site I obtained from HADDOCK calculations.

The results are in agreement with the NMR spectroscopic data, supporting the NMR observation of the predominant interactions of $[\text{VO}_2(\text{dmpp})(\text{H}_2\text{O})(\text{OH})]^-$ and $[\text{VO}_2(\text{maltol})_2]^-$ complexes with HSA, as shown by the relatively low HADDOCK score for these species. The protein residues close to and interacting with the small molecules remain conserved in all the calculations, which reflects the consistency of the results. As shown in Figure 5, the aromatic moiety is in close proximity to the hydrophobic resi-

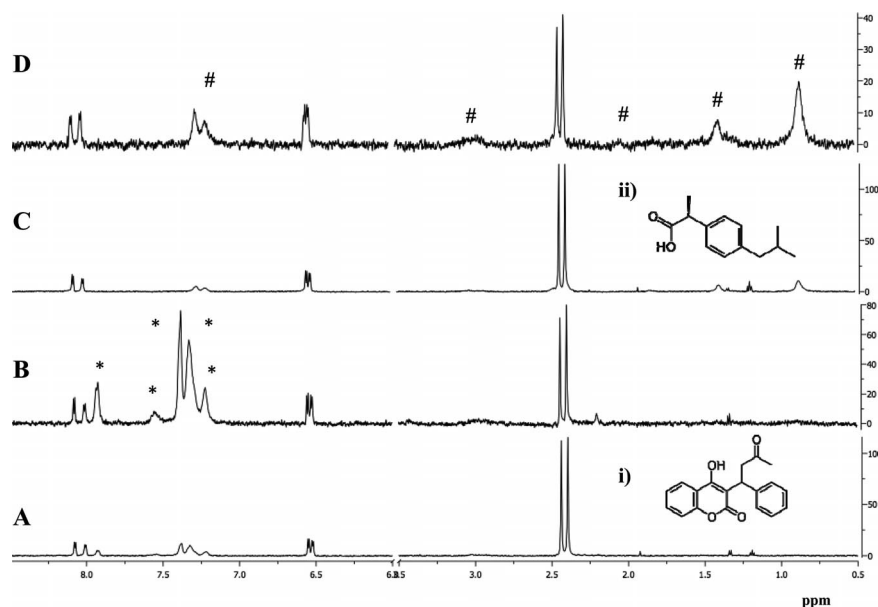


Figure 4. ^1H NMR spectra of A) a solution containing vanadate/maltol (1:2, 1 mM in vanadate) and 0.03 mM HSA to which 0.1 mM warfarin (structure i)) has been added, B) the STD spectrum of the same solution as in A, C) a solution of vanadate/maltol (1:2, 1 mM in vanadate) and 0.03 mM HSA to which 0.4 mM ibuprofen (structure ii) has been added and D) the STD spectrum of the same solution as in C. A selective saturation pulse (5 s) was applied to the 0 ppm region of the protein. A 30 ms spin-lock pulse was calibrated to avoid unwanted protein resonances. Competitor resonances are indicated by * (warfarin) and # (ibuprofen). The difference in the vertical scale of the reference (A,C) and STD (B,D) spectra is due to the difference in the number of scans used in the respective acquisitions (see the Exp. Sect.).

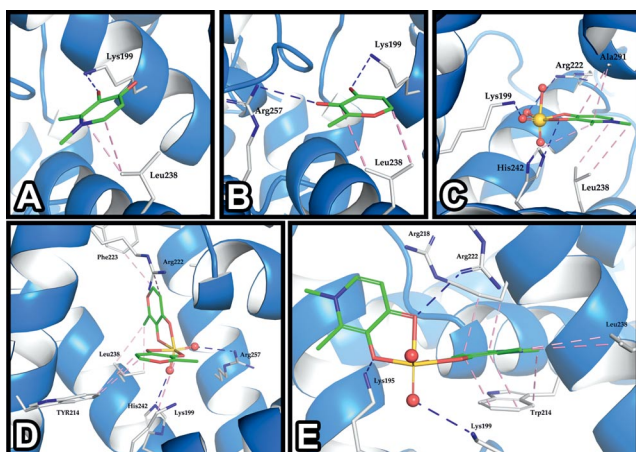


Figure 5. HADDOCK models for the interaction of HSA (warfarin pocket, drug site I) with small molecules: A) the free ligand Hdmpp, B) the free ligand maltol, C) $[\text{VO}_2(\text{dmpp})_2]^-$, D) $[\text{VO}_2(\text{maltolato})_2]^-$ and E) $[\text{VO}_2(\text{dmpp})(\text{OH})(\text{H}_2\text{O})]^-$. The main interacting residues are shown by stick representation and electrostatic and van der Waals interactions are represented by blue and pink dashed lines, respectively. The figures were drawn with PyMOL.

dues (L238, F223, W214), namely L238, which is present in all the modelled compounds. For the $[\text{VO}_2(\text{dmpp})(\text{H}_2\text{O})(\text{OH})]^-$ species, the model shows a large number of hydrophobic interactions with the planar ring, which con-

tributes to its greater stability when compared with the other species. The binding of the small molecules to the protein is also stabilized by electrostatic interactions, mainly with K199 and H242, but also with other positively charged residues (K195, R222, R257). The binding site of the maltol and dmpp V^{V} complexes differs slightly. Although the R222 residue interacts directly with the V^{V} species in the dmpp complexes, in $[\text{VO}_2(\text{maltol})_2]^-$ this residue is replaced by R257, showing a different orientation of the small molecule, which may be attributed to the higher bulk effect of the aromatic moiety of dmpp. The two larger V^{V} complexes, with an M/L ratio of 1:2, seem to displace a large number of protein side-chains, establishing interactions with residues lying deeper in the pocket (e.g., Y214). The $[\text{VO}_2(\text{dmpp})_2]^-$ species is found in the majority of the models in a very different binding position, located at the surface of the protein. This is likely because the larger dmpp moiety cannot be accommodated in the binding pocket without severe steric hindrance from the protein side-chains, which may explain the lower binding affinity. Even for the small set of solutions (Table 3, small cluster of $[\text{VO}_2(\text{dmpp})_2]^-$) that penetrate the pocket of HSA site I, there are no stabilizing interactions between the protein and the second dmpp moiety, which is in support of steric effects. For $[\text{VO}_2(\text{maltolato})_2]^-$, both maltolato moieties are stabilized by hydrophobic interactions with residues Y214, F223, R222 and L238, as well as the above-mentioned electrostatic interactions, conferring a higher affinity of this V^{V} species on the binding pocket compared with uncoordinated maltol.

Table 3. Results of HADDOCK calculations from the top ranking clusters after water refinement for each compound in their interaction with HSA. The HADDOCK score, energies of van der Waals and electrostatic interactions and buried surface area (BSA) were obtained from the docking calculations automatic analysis.

	Hdmpp	[VO ₂ (dmpp)(H ₂ O)(OH)] ⁻	[VO ₂ (dmpp) ₂] ⁻		Maltol	[VO ₂ (maltol) ₂] ⁻
Cluster size	257	219	4	196	153	59
Haddock score [a.u.]	15.9 ± 3.5	-8.8 ± 1.8	12.0 ± 11.9	23.8 ± 3.7	24.9 ± 0.4	2.6 ± 1.8
van der Waals [kcal/mol]	-11.1 ± 2.9	-166.8 ± 16.9	-104.1 ± 2.8	-21.3 ± 12.9	-19.4 ± 4.3	-61.6 ± 6.3
Electrostatic [kcal/mol]	-19.3 ± 0.8	-26.7 ± 1.1	-30.5 ± 2.0	-23.8 ± 0.7	-15.6 ± 1.2	-30.8 ± 0.6
BSA [Å ²]	324.7 ± 27.7	496.3 ± 14.9	736.3 ± 20.6	461.2 ± 9.1	295.8 ± 16.9	711.8 ± 6.7

Conclusions

The results presented in this work show that the species that result from the dissolution and oxidation of [V^{IV}O-(dmpp)₂], a vanadium compound that has demonstrated promising anti-diabetic and anti-obesity ability, bind to HSA, the most abundant protein in blood plasma. Similar results were obtained with the species originating from the dissolution and oxidation of the well-known [V^{IV}O-(maltolato)₂] (BMOV) complex, which is already in clinical trials. The ¹H STD NMR technique has provided valuable information concerning the binding of these VCs to HSA. Competitive STD NMR experiments revealed that site I of HSA is the main site involved in this binding. Thus, HSA appears to be an important vehicle for the transport of vanadium species once in the blood stream and their delivery to target cells. The molecular docking studies supported by the NMR spectroscopic data indicate a preference for the binding of 1:1 [VO(dmpp)(H₂O)(OH)]⁻ to HSA site I relative to the 1:2 [VO₂(dmpp)₂]⁻ complex, as shown by the lower HADDOCK score. The binding of [VO₂-(maltolato)₂]⁻ to this site is also favoured over free maltol.

The ¹H STD NMR technique has proven to be a useful tool for studying the interactions of these V^V complexes with HSA. In addition, the docking simulations of these interactions complement the STD NMR spectroscopic data, allowing the interaction of metal-coordinated systems with macromolecules to be modelled with high resolution, an important issue in this field of research. Together, the results presented in this work contribute to a better understanding of the fate of VCs and their derivatives after their administration and once in the blood stream.

Experimental Section

Reagents and Solutions: Sodium metavanadate, NaVO₃ (99.9%), 3-hydroxy-1,2-dimethyl-4-pyridinone (Hdmpp), 3-hydroxy-2-methyl-4-pyrone (maltol, 99%), human serum albumin (HSA), ibuprofen, warfarin, D₂O (99.6% D), DCl (wt. 35%, 99% D) and NaOD (wt. 30%, 99% D) were purchased from Sigma–Aldrich. All reagents were used without further purification.

Stock solutions of HSA (1 mM), ibuprofen (2 mM), warfarin (2 mM), vanadate (6 mM), Hdmpp (60 mM) and maltol (60 mM) were prepared in D₂O. Solutions containing vanadate and Hdmpp in M/L ratios of 1:2, 1:2.5 and 1:5 were prepared by adding the appropriate volumes of metal and ligand stock solutions. The vanadate/maltol solutions in M/L ratios of 1:2, 1:5 and 1:20 were prepared similarly. Samples containing HSA (30 μM) and vanadate/dmpp or vanadate/maltolato (500 μM in vanadate), in different M/L ratios were ana-

lysed by ¹H NMR spectroscopy. In all cases a large excess of the V^V complex relative to the protein was used as required by the STD protocol.

Competition studies were performed with warfarin and ibuprofen, two known binders of site I and site II of HSA, respectively.^[50] Samples containing HSA (30 μM), vanadate/dmpp or vanadate/maltolato solutions (500 μM in vanadate and in an M/L ratio of 1:2.5) and ibuprofen (400 μM) or warfarin (100 μM) were analysed.

The pH of all the solutions was adjusted to the physiological value (pH 7–7.4) by using DCl or NaOD, and measured with a pH meter equipped with a combined pH electrode Sentek P13/S7. The pH values were not corrected for the isotopic effect.

¹H NMR Spectroscopy: ¹H NMR spectra were recorded with a Varian VNMRs 600 NMR spectrometer operating at 599.72 MHz by using a pulse field gradient (PFG) inverse 3 mm probe at 298 K. The pulse sequence for the ¹H NMR STD spectra acquisition^[51] used a double pulse field gradient spin echo (DPFGSE) to efficiently remove the water signal. The NMR spectrometer used acquired the STD NMR spectra directly from phase cycling to calculate the STD amplification factor and the 1D ¹H NMR spectra were used as off-resonance reference spectra. All the spectra were acquired by using the following parameters: spectral width of 8 kHz, number of transients 128 for 1D ¹H and 1024 for ¹H STD NMR spectra, acquisition time of 2 s and repetition time of 5 s. A previously calibrated spin-lock filter (*T*_{1ρ}) of 30 ms was used to remove protein resonances. The difference in the number of transients used for the reference 1D and STD ¹H NMR spectra was corrected through normalization according to the Equation (1) in which *I*_{STD} is the intensity of a signal in the STD NMR spectrum and *I*₀ is its intensity in the 1D ¹H NMR reference spectrum.

$$\text{Rel. STD\%} = \frac{I_{\text{STD}} \times 2 \times \text{scans}_{\text{reference}}}{I_0 \times \text{scans}_{\text{STD}}} \quad (1)$$

The STD amplification factor (*A*_{STD}) was determined according to Equation (2) in which the “small molecule (SM) excess” is the ratio [SM]/[P], with [SM] as the total concentration of the V^V coordinated species and [P] is the total protein concentration.

$$A_{\text{STD}} = \text{Rel. STD\%} \times \text{SM}_{\text{excess}} \quad (2)$$

Group epitope mapping (GEM) values were obtained for each proton by normalizing the *A*_{STD} values of all protons of the SM to the proton presenting the highest STD effect. All the spectra were processed and analysed by using the Mestre Nova software.^[58]

Protein–Small-Molecule Docking Studies: To provide a more detailed insight into the binding mode, HADDOCK was used^[47,48] to derive a model of the interaction. The crystal structure of the complex of HSA with warfarin (PDB ID: 2BXD)^[52] was selected as a representative structure for HSA because competition experiments show a preferential interaction of the small molecules with the warfarin binding site.

The 3D structures of the small molecules, Hdmpp, maltol and their respective V^V -coordinated species, were generated by using a hybrid parametrization scheme as the complexes contain an unusual vanadium metal atom and a high number of bonds (six) to this central atom. To assign charges and geometric parameters for the aromatic moieties, a semi-empirical quantum chemistry package (SQM, part of the AmberTools package^[53]) through the wrapper ACPYPE^[54] with default settings, except for the net charge that depends on the binding molecule (neutral for Hdmpp and maltol, -1 for their respective V^V coordinated species). This software uses AM1-BCC parameters, tuned to reproduce HF/6-31G* RESP charges for partial charge calculations. The semi-empirical character of the calculations provides reasonable parametrization accuracy within a few minutes.

The $V^V O_2^+$ metal centre was manually parametrized by using the geometrical features characterized by Caravan et al. for complexes with maltol.^[49] The 1:1 octahedral V^V species coordinate two water molecules, one of which is deprotonated at physiological pH and was thus represented accordingly. To avoid artifacts due to the highly charged vanadate ion, the total charge of the intervening atoms was reduced while keeping the same ratio and net charge (+1).

The docking was performed with HADDOCK version 2.2^[47,48] by using CNS1.3^[55] for the structure calculations as this software allows the integration of biochemical and/or biophysical information to drive the modelling. The docking protocol consists of three steps: 1) rigid body docking, 2) semi-flexible refinement by using a simulated annealing protocol in torsion angle space and 3) final refinement in explicit water. Non-bonding interactions were calculated with the OPLS force field^[56] using a cut-off at 8.5 Å. The electrostatic potential (E_{elec}) was calculated by means of a shift function, and a switching function, between 6.5 and 8.5 Å, was used for the van der Waals potential (E_{vdw}). The HADDOCK score was used to rank the generated models. It consists of a weighted sum of intermolecular electrostatic, van der Waals, desolvation (ΔG_{solv})^[57] and ambiguous interaction restraint (AIR) energies, defined in Equation (3).

$$\text{Haddock score} = 0.2E_{elec} + 1.0E_{vdw} + 1.0E_{\Delta G_{solv}} + 0.1E_{AIR} \quad (3)$$

The ambiguous interaction restraints used to drive the docking were defined as follows: 1) the small molecule was always treated as an active residue, 2) for the 1:2 species, considering their symmetrical conformation, only one of the ligands was considered active, 3) the residues of the HSA binding site were considered as active only during the rigid-body docking stage whereas for the remainder of the docking protocol they were defined as passive. This effectively pulls the ligand molecule to the appropriate site of the protein during rigid-body docking while allowing a more relaxed exploration of the binding pocket during the refinement stage. The binding site of 2BXD is defined as the residues at around 5 Å from the warfarin molecule: 150, 195, 199, 211, 214, 215, 218, 219, 222, 238, 241, 242, 257, 260, 261, 264, 290, 291, 292. The GEM data was incorporated as ambiguous distance restraints during the semi-flexible and water refinement stages. The carbon atoms bonded to the 5-H/6-H protons were required to be within 4 Å of any residue in the binding pocket.

The docking was performed with default HADDOCK settings, except for the following parameters: 1) the number of structures generated in the three stages of the docking protocol increased to 5000/400/400, 2) all hydrogen atoms were kept, 3) the random exclusion of a fraction of the AIRs was disabled, 4) the random exclusion of a fraction of the AIRs was disabled, 5) the number of molecular

dynamics steps for both rigid-body high-temperature torsion angle dynamics (TAD) and the rigid-body cooling stage were set to zero to avoid expulsion of the ligand from the pocket, 6) the initial temperature for the second TAD cooling step was reduced to 500 K, for the same reason as the previous and 7) the clustering cut-off for the final solutions was reduced to 1 Å instead of the default 7.5 Å, as is adequate for a small ligand.

Supporting Information (see footnote on the first page of this article): Details about the drug sites I and II of HSA mentioned in this work, the warfarin and ibuprofen binding sites, respectively, why they were chosen for this study, their localization in the protein and structural features.

Acknowledgments

Financial support by the Portuguese Fundação para a Ciência e Tecnologia (FCT) within the Programa Nacional de Equipamento Científico Varian (contract number REDE/1517/RMN/2005) as part of the Portuguese-NMR network (Rede Nacional de RMN) is acknowledged. D. M. D. thanks the The European NMR Large Scale Facility Utrecht for the contact with SONNMRSLF (project number BIO-NMR-00041). A. M. J. J. B. and J. R. acknowledge funding from the Dutch Foundation for Scientific Research (NWO) (VICI grant number 700.56.442) and Utrecht University (Focus and Massa grant). The authors would like to thank Dr. M. H. Weingarth and the members of the HADDOCK group for helpful discussions and Prof. Dr. João Costa Pessoa and his post-doc student Somnath Roy at the Technical University of Lisbon, Portugal, for the synthesis of the vanadium compounds.

- [1] H. Sakurai, Y. Yoshikawa, H. Yasui, *Chem. Soc. Rev.* **2008**, *37*, 2383–2392.
- [2] H. Sakurai, K. Fujii, H. Watanabe, H. Tamura, *Biochem. Biophys. Res. Commun.* **1995**, *214*, 1095–1101.
- [3] H. Sakurai, H. Sano, T. Takino, H. Yasui, *J. Inorg. Biochem.* **2000**, *80*, 99–105.
- [4] K. Kawabe, Y. Yoshikawa, Y. Adachi, H. Sakurai, *Life Sci.* **2006**, *78*, 2860–2866.
- [5] Y. Schechter, *Lett. Pept. Sci.* **1998**, *5*, 319–322.
- [6] M. Hiromura, A. Nakayama, Y. Adachi, M. Doi, H. Sakurai, *J. Biol. Inorg. Chem.* **2007**, *12*, 1275–1287.
- [7] K. H. Thompson, J. H. McNeill, C. Orvig, *Chem. Rev.* **1999**, *99*, 2561–2571.
- [8] W. Basuki, M. Hiromura, Y. Adachi, K. Tayama, M. Hattori, H. Sakurai, *Biochem. Biophys. Res. Commun.* **2006**, *349*, 1163–1170.
- [9] V. G. Yuen, C. Orvig, J. H. McNeill, *Can. J. Physiol. Pharmacol.* **1993**, *71*, 263–269.
- [10] M. Hiromura, A. Nakayama, Y. Adachi, M. Doi, H. Sakurai, *J. Biol. Inorg. Chem.* **2007**, *12*, 1275–1287.
- [11] M. Hiromura, H. Sakurai, *Chem. Biodiversity* **2008**, *5*, 1615–1621.
- [12] Z. W. Yu, P. A. Jansson, B. I. Posner, U. P. Smith, J. W. Eriksson, *Diabetologia* **1997**, *40*, 1197–1203.
- [13] W. M. Mueller, K. L. Stanhope, F. Gregoire, J. L. Evans, P. J. Havel, *Obes. Res.* **2000**, *8*, 530–539.
- [14] Y. Adachi, H. Sakurai, *Chem. Pharm. Bull.* **2004**, *52*, 428–433.
- [15] J. Gätjens, B. Meier, T. Kiss, E. M. Nagy, P. Buglyó, H. Sakurai, K. Kawabe, D. Rehder, *Chem. Eur. J.* **2003**, *9*, 924–935.
- [16] H. Faneca, V. A. Figueiredo, I. Tomaz, G. Gonçalves, F. Avecilla, M. C. Pedroso de Lima, C. F. G. C. Geraldes, J. C. Pessoa, M. M. C. A. Castro, *J. Inorg. Biochem.* **2009**, *103*, 601–608.
- [17] D. C. Crans, *J. Inorg. Biochem.* **2000**, *80*, 123–131.
- [18] K. H. Thompson, J. Lichter, C. LeBel, M. C. Scaife, J. H. McNeill, C. Orvig, *J. Inorg. Biochem.* **2009**, *103*, 554–558.

- [19] J. Burgess, B. Castro, C. Oliveira, M. Rangel, W. Schlindwein, *Polyhedron* **1997**, *16*, 789.
- [20] M. M. C. A. Castro, F. Avecilla, C. F. G. C. Geraldés, B. de Castro, M. Rangel, *Inorg. Chim. Acta* **2003**, *356*, 142–154.
- [21] D. Rehder, J. C. Pessoa, C. F. G. C. Geraldés, M. M. C. A. Castro, T. Kabanos, T. Kiss, B. Meier, G. Micera, L. Pettersson, M. Rangel, A. Salifoglou, I. Turel, D. Wang, *J. Biol. Inorg. Chem.* **2002**, *7*, 384–396.
- [22] T. C. Delgado, I. Correia, J. C. Pessoa, J. G. Jones, C. F. G. C. Geraldés, M. M. C. A. Castro, *J. Inorg. Biochem.* **2005**, *99*, 2328–2339.
- [23] M. Passadouro, A. M. Metelo, A. S. Melão, J. R. Pedro, H. Faneca, E. Carvalho, M. M. C. A. Castro, *J. Inorg. Biochem.* **2010**, *104*, 987–992.
- [24] A. M. Metelo, R. Pérez-Carro, M. M. C. A. Castro, P. López-Larrubia, *J. Inorg. Biochem.* **2012**, *115*, 44–49.
- [25] K. H. Thompson, C. Orvig, *J. Chem. Soc., Dalton Trans.* **2000**, 2885–2892.
- [26] T. Takino, H. Yasui, A. Yoshitake, Y. Hamajima, R. Matsushita, J. Takada, H. Sakurai, *J. Biol. Inorg. Chem.* **2001**, *6*, 133–142.
- [27] T. Kiss, T. Jakusch, D. Hollender, Á. Dörnyei, É. A. Enyedy, J. C. Pessoa, H. Sakurai, A. Sanz-Medel, *Coord. Chem. Rev.* **2008**, *252*, 1153–1162.
- [28] B. D. Liboiron, K. H. Thompson, G. R. Hanson, E. Lam, N. Aebischer, C. Orvig, *J. Am. Chem. Soc.* **2005**, *127*, 5104–5115.
- [29] D. Sanna, G. Micera, E. Garribba, *Inorg. Chem.* **2009**, *48*, 5747–5757.
- [30] D. Sanna, G. Micera, E. Garribba, *Inorg. Chem.* **2010**, *49*, 174–187.
- [31] D. Sanna, P. Buglyo, G. Micera, E. Garribba, *J. Biol. Inorg. Chem.* **2010**, *15*, 825–839.
- [32] I. Correia, T. Jakusch, E. Cobbinna, S. Mehtab, I. Tomaz, N. V. Nagy, A. Rockenbauer, J. Costa Pessoa, T. Kiss, *J. Chem. Soc., Dalton Trans.* **2012**, *41*, 6477–6487.
- [33] P. Buglyó, T. Kiss, E. Kiss, D. Sanna, E. Garribba, G. Micera, *J. Chem. Soc., Dalton Trans.* **2002**, 2275–2282.
- [34] T. Jakusch, A. Dean, T. Oncsik, A. C. Benyei, V. Di Marcob, T. Kiss, *Dalton Trans.* **2010**, *39*, 212–220.
- [35] a) C. C. Chéry, K. de Cremer, E. Dumont, R. Cornelis, L. Moens, *Electrophoresis* **2002**, *23*, 3284–3288; b) K. de Cremer, M. van Hulle, C. C. Chéry, R. Cornelis, K. Strijkmans, R. Dams, N. Lameire, R. Vanholder, *J. Biol. Inorg. Chem.* **2002**, *7*, 884–890.
- [36] a) M. H. Nagaoka, T. Yamazaki, T. Maitani, *Biochem. Biophys. Res. Commun.* **2002**, *296*, 1207–1214; b) G. Heinemann, B. Fichtl, M. Mentler, W. Vogt, *J. Inorg. Biochem.* **2002**, *90*, 38–42.
- [37] E. G. Ferrer, A. Bosch, O. Yantorno, E. J. Baran, *Bioorg. Med. Chem.* **2008**, *16*, 3878–3886.
- [38] a) A. Butler, M. J. Danzitz, *J. Am. Chem. Soc.* **1987**, *109*, 1864–1865; b) A. Butler, H. Eckert, *J. Am. Chem. Soc.* **1989**, *111*, 2802–2809; c) J. A. Saponja, H. J. Vogel, *J. Inorg. Biochem.* **1996**, *62*, 253–270; d) D. Rehder, M. Časný, R. Grosse, *Magn. Reson. Chem.* **2004**, *42*, 745–749.
- [39] a) J. C. Cannon, N. D. Chasteen, *Biochemistry* **1975**, *14*, 4573–4577; b) R. Campbell, N. D. Chasteen, *J. Biol. Chem.* **1977**, *252*, 5996–6001.
- [40] N. D. Chasteen, J. Francavilla, *J. Phys. Chem.* **1976**, *80*, 867–871.
- [41] a) N. D. Chasteen, J. K. Grady, C. E. Holloway, *Inorg. Chem.* **1986**, *25*, 2754–2760; b) G. R. Wilsky, A. B. Goldfine, P. J. Kostyniak, J. H. McNeill, L. Q. Yang, H. R. Lan, D. C. Crans, *J. Inorg. Biochem.* **2001**, *85*, 33–42; c) A.-K. Boardbar, A. L. Creagh, F. Mohammadi, C. A. Haynes, C. J. Orvig, *J. Inorg. Biochem.* **2009**, *103*, 643–647.
- [42] T. Kiss, E. Kiss, E. Garriba, H. Sakurai, *J. Inorg. Biochem.* **2000**, *80*, 65–73.
- [43] T. Jakusch, D. Hollender, É. A. Enyedy, C. S. Gonzáles, M. Montes-Bayón, A. Sanz-Medel, J. C. Pessoa, I. Tomaz, T. Kiss, *Dalton Trans.* **2009**, 2428–2437.
- [44] H. Sakurai, S. Shimomura, K. Fukazawa, K. Ishizu, *Biochem. Biophys. Res. Commun.* **1980**, *96*, 293–298.
- [45] M. Mayer, B. Meyer, *Angew. Chem.* **1999**, *111*, 1902; *Angew. Chem. Int. Ed.* **1999**, *38*, 1784–1788.
- [46] D. M. Dias, J. M. C. Teixeira, I. Kuprov, E. J. New, D. Parker, C. F. G. C. Geraldés, *Org. Biomol. Chem.* **2011**, *9*, 5047–5050.
- [47] C. Dominguez, R. Boelens, A. M. Bonvin, *J. Am. Chem. Soc.* **2003**, *125*, 1731–1737.
- [48] S. J. de Vries, A. S. Melquiond, P. L. Kastiris, E. Karaca, A. Bordogna, M. van Dijk, J. P. Rodrigues, A. M. Bonvin, *Proteins* **2010**, *78*, 3242–3249.
- [49] P. Caravan, L. Gelmini, N. Glover, F. G. Herring, H. L. Li, J. H. McNeill, S. J. Rettig, I. A. Setyawatti, E. Shuter, Y. Sun, A. S. Tracey, V. G. Yuen, C. J. Orvig, *J. Am. Chem. Soc.* **1995**, *117*, 12759–12770.
- [50] T. Peters Jr., *All About Albumin*, Academic Press, San Diego, CA, **1996**.
- [51] a) Y. S. Wang, D. Liu, D. F. Wyss, *Magn. Reson. Chem.* **2004**, *42*, 485–489; b) T.-L. Hwang, A. J. Shaka, *J. Magn. Reson., Ser. A* **1995**, *112*, 275–279.
- [52] J. Ghuman, P. A. Zunsain, I. Petitpas, A. A. Bhattacharya, M. Otagiri, S. Curry, *J. Mol. Biol.* **2005**, *353*, 38–52.
- [53] J. Wang, R. M. Wolf, J. W. Caldwell, P. A. Kollman, D. A. Case, *J. Comput. Chem.* **2004**, *25*, 1157–1174.
- [54] A. W. Sousa da Silva, W. F. Vranken, ACPYPE – AnteChamber PYthon Parser InterfacE, *BMC Res. Notes* **2012**, *5*, 367.
- [55] A. T. Brünger, P. D. Adams, G. M. Clore, W. L. DeLano, P. Gros, R. W. Grosse-Kunstleve, J. S. Jiang, J. Kuszewski, M. Nilges, N. S. Pannu, R. J. Read, L. M. Rice, T. Simonson, G. L. Warren, *Acta Crystallogr., Sect. D* **1998**, *54*, 905–921.
- [56] W. Jorgensen, J. Tirado-Rives, *J. Am. Chem. Soc.* **1988**, *110*, 1657–1666.
- [57] J. Fernández-Recio, M. Totrov, R. Abagyan, *J. Mol. Biol.* **2004**, *335*, 843–865.
- [58] *MestRe Nova*, v5.3.1-4825, Mestrelab Research S.L., Santiago de Compostela, Spain.

Received: March 29, 2013
Published Online: July 19, 2013